Homework 4 Computational Physics

Giacomo Recine*

11 November 2025

Contents

*gr2640@nyu.edu

1 Introduction

In this homework, we will implement the fourth-order Runge–Kutta method with adaptive step size, which is necessary for our physical system. In Sec. 2, we perform a simulation of the three-body problem, focusing on the so-called Moore–Chenciner–Montgomery configuration, where the motion becomes periodic. In Sec. 3, we apply the same method to compute the orbit of a supermassive black hole around another, both with and without dynamical drift. We will analyze how the time required to reach the so-called Schwarzschild radius depends on the parameters of the dynamical drift term, and how it changes with different initial velocities.

2 Exercise 8.18: Simulation of the Three Body Problem

In this exercise, we will perform a two dimensional simulation of the motion of a three body system subjected to gravitational attraction. To do this, we solve the second order differential equations using the fourth order Runge-Kutta method. Since we will use the same method in the second part of this homework, we will first explain how this integration method works.

2.1 Runge-Kutta method

Taking a first order differential equation, like

$$\frac{dx}{dt} = f(x,t), \tag{1}$$

we can solve it by considering the so called Runge Kutta algorithm. For the fourth order Runge Kutta method, the solution is advanced from t to $t+h$ as follows:

$$k_1 = f(x,t), \tag{2}$$

$$k_2 = f\left(x + \frac{h}{2}k_1,\, t + \frac{h}{2}\right), \tag{3}$$

$$k_3 = f\left(x + \frac{h}{2}k_2,\, t + \frac{h}{2}\right), \tag{4}$$

$$k_4 = f\left(x + h\,k_3,\, t + h\right), \tag{5}$$

and the new value of x is obtained from

$$x(t+h) = x(t) + \frac{h}{6}\left(k_1 + 2k_2 + 2k_3 + k_4\right). \tag{6}$$

This method provides a good balance between accuracy and computational efficiency, and it is one of the most commonly used algorithms for solving ordinary differential equations numerically.

Of course, there is the possibility of having more than one variable. In that case, defining the vector $\mathbf{r} = (x, y, \ldots)$, the system of equations can be written as

$$\frac{d\mathbf{r}}{dt} = \mathbf{f}(\mathbf{r},t), \tag{7}$$

and the fourth order Runge Kutta method takes the following vector form

$$\mathbf{k}_1 = \mathbf{f}(\mathbf{r},t), \tag{8}$$

$$\mathbf{k}_2 = \mathbf{f}\left(\mathbf{r} + \frac{h}{2}\mathbf{k}_1,\, t + \frac{h}{2}\right), \tag{9}$$

$$\mathbf{k}_3 = \mathbf{f}\left(\mathbf{r} + \frac{h}{2}\mathbf{k}_2,\, t + \frac{h}{2}\right), \tag{10}$$

$$\mathbf{k}_4 = \mathbf{f}\left(\mathbf{r} + h\,\mathbf{k}_3,\, t + h\right), \tag{11}$$

and the new value of the vector $\mathbf{r}$ is obtained from

$$\mathbf{r}(t+h) = \mathbf{r}(t) + \frac{h}{6}\left(\mathbf{k}_1 + 2\mathbf{k}_2 + 2\mathbf{k}_3 + \mathbf{k}_4\right). \tag{12}$$

This vector formulation allows the method to be applied easily to systems of ordinary differential equations, such as those describing the motion of particles in two or three dimensions under mutual gravitational attraction.

As said anyway this method can be applied for the first order differential equation. And what about the second order differential equation? To solve this type we need to use a very useful trick, which is the following. Let's consider directly the most general case with more variables. Thus a set of simultaneous second-order equations can be written in vector form as

$$\frac{d^2\mathbf{r}}{dt^2} = \mathbf{f}\left(\mathbf{r}, \frac{d\mathbf{r}}{dt}, t\right), \tag{13}$$

but considering the system of first-order equations

$$\frac{d\mathbf{r}}{dt} = \mathbf{s}, \qquad \frac{d\mathbf{s}}{dt} = \mathbf{f}(\mathbf{r}, \mathbf{s}, t), \tag{14}$$

we have now a single second-order differential equations. If we started instead with two simultaneous second-order equations, we would obtain, after applying the same transformation, a system of four simultaneous first-order equations. More generally, an initial system of n equations of order m can be transformed into an equivalent system of $m \times n$ simultaneous first-order equations, which can then be solved using the standard methods for systems of first-order differential equations.

Now we are ready to use these techniques to solve our problems.

2.2 Solution of the Exercise

2.2.1 Question a

For the three-body problem, we have the following three equations

$$\frac{d^2\mathbf{r}_1}{dt^2} = Gm_2\frac{\mathbf{r}_2 - \mathbf{r}_1}{\|\mathbf{r}_2 - \mathbf{r}_1\|^3} + Gm_3\frac{\mathbf{r}_3 - \mathbf{r}_1}{\|\mathbf{r}_3 - \mathbf{r}_1\|^3}, \tag{15}$$

$$\frac{d^2\mathbf{r}_2}{dt^2} = Gm_1\frac{\mathbf{r}_1 - \mathbf{r}_2}{\|\mathbf{r}_1 - \mathbf{r}_2\|^3} + Gm_3\frac{\mathbf{r}_3 - \mathbf{r}_2}{\|\mathbf{r}_3 - \mathbf{r}_2\|^3}, \tag{16}$$

$$\frac{d^2\mathbf{r}_3}{dt^2} = Gm_1\frac{\mathbf{r}_1 - \mathbf{r}_3}{\|\mathbf{r}_1 - \mathbf{r}_3\|^3} + Gm_2\frac{\mathbf{r}_2 - \mathbf{r}_3}{\|\mathbf{r}_2 - \mathbf{r}_3\|^3}. \tag{17}$$

Now starting from the last equations, we can write directly the following second-order equations

$$m_i\frac{d^2\mathbf{r}_i}{dt^2} = \sum_{\substack{j=1 \\ j\neq i}}^{3} G\, m_i m_j \frac{\mathbf{r}_j - \mathbf{r}_i}{|\mathbf{r}_j - \mathbf{r}_i|^3}, \qquad i = 1, 2, 3. \tag{18}$$

As explained in the previous section, we can convert the three second-order equations into six equivalent first-order equations by introducing new variables for the velocities. Indeed

- step 1: define the velocity vectors

$$\mathbf{v}_i = \frac{d\mathbf{r}_i}{dt}, \qquad i = 1, 2, 3. \tag{19}$$

- step 2: rewrite the system as first-order equations

$$\frac{d\mathbf{r}_i}{dt} = \mathbf{v}_i, \tag{20}$$

$$\frac{d\mathbf{v}_i}{dt} = G\sum_{\substack{j=1\\ j\neq i}}^{3} m_j \frac{\mathbf{r}_j - \mathbf{r}_i}{|\mathbf{r}_j - \mathbf{r}_i|^3}, \qquad i = 1, 2, 3. \tag{21}$$

Hence, the original system of three second-order equations has been transformed into a system of six first order differential equations, three for the positions $\mathbf{r}_i$ and three for the velocities $\mathbf{v}_i$.

2.2.2 Questions b and c

Now taking $G = 1$, we write a code that solve our equations and hence calculate the motion of the stars from $t = 0$ to $t = 10$, and in the end we will make an animation of the motion. For the code used to solve our equations, we implemented the Runge Kutta method described in Eq. (8), but with an adaptive time step, which we will now explain. The numerical methods introduced so far use a fixed step size h, chosen in advance by the programmer. However, in many situations, better accuracy and efficiency can be achieved by allowing the step size to vary during the integration, letting the program choose the most appropriate value at each step. When the solution varies slowly, a larger step can be used without loss of precision, while in regions where the function changes rapidly, smaller steps are required. This approach allows us to obtain an accurate solution using fewer total points, thus improving computational efficiency and this technique is known as the adaptive step size method. Its main idea is to adjust h dynamically so that the numerical error per unit time remains approximately constant throughout the integration. In practice, the adaptive step size method consists of two main parts. First, we estimate the error at each integration step. Then, we compare this estimated error with the desired accuracy and adjust the step size accordingly, either increasing or decreasing it to achieve the required precision. The following describes how this approach is applied to the fourth order Runge Kutta method.

So practically is computed the following quantity

$$\rho = \frac{30h\delta}{|x_1 - x_2|} \tag{22}$$

where the target accuracy per unit time for our calculation is δ, which means that the target accuracy for a single step of size h' would be $h'\delta$.

The complete method proceeds as follows. We first perform two integration steps, each of size h. Then, starting again from the same initial point, we perform a single step of size $2h$. This procedure provides two independent estimates, x_1 and x_2, of the solution $x(t + 2h)$. We then compute the ratio ρ defined in Eq. (22). If $\rho > 1$, this indicates that the actual accuracy of our Runge–Kutta steps is higher than the target accuracy. In other words, the calculation satisfies the accuracy requirement, but it is inefficient because the step size used is smaller than necessary. In this case, we accept the results and proceed to time $t + 2h$ to continue the integration, but we increase the step size in the next iteration to improve computational efficiency and avoid unnecessary computation. Conversely, if $\rho < 1$, the actual accuracy of the calculation is lower than the target accuracy, meaning that the current step has failed. In this case, the step must be repeated with a smaller step size, as determined by Eq. (22). After each iteration, depending on the value of ρ, we either increase h and proceed to the next step, or decrease h and repeat the current one. For the actual solution of the differential equation, we always use the estimate x_1, since it is obtained with the smaller step size and is therefore more accurate. The estimate x_2, computed with the larger step, is used only for error estimation and step size adjustment, not for the final solution.

Three stars, located in otherwise empty space, are initially at rest. Their masses and initial positions (in arbitrary units) are given as follows

Table 1: Initial conditions for the three-body system.

Star	Mass	Initial Position (x, y)	Initial Velocity (v_x, v_y)
Star 1	150	(3, 1)	(0.0, 0.5)
Star 2	200	$(-1, -2)$	(0.5, 0.0)
Star 3	250	$(-1, 1)$	(-0.5, -0.5)

We then computed the motion of the stars over the time interval from $t = 0$ to $t = 10$. Using the `qdraw.py` library, and setting $G = 1$ we created an animation showing their trajectories with visible trails (see the code provided in Sec. 5).

Examining the animation, we observe that, for the initial conditions used above, the motion of the three stars is aperiodic and unpredictable. This behavior is typical of the three-body problem, which is known for its sensitivity to initial conditions and chaotic dynamics. For instance, at $t = 10$ we obtain the following final positions of the three stars

Figure 1: Plot of the final trajectories of the stars for the chosen initial conditions.

However, there exist remarkable exceptions. In 1993, physicist Christopher Moore discovered a stable, periodic orbit in which three bodies move around one another in a continuous loop. This discovery was first made using computational methods and was later confirmed analytically by Alain Chenciner and Richard Montgomery. In the Moore-Chenciner-Montgomery orbit, all three stars have the same mass, which we set to $m = 1$. Their initial positions and velocities are given by

Table 2: Initial conditions for the Moore-Chenciner-Montgomery three-body orbit.

Star	Mass	Initial Position (x, y)	Initial Velocity (v_x, v_y)
Star 1	1	$(0, \quad 0)$	$(0.93240737, \quad 0.86473146)$
Star 2	1	$(0.97000436, \quad -0.24308753)$	$(-0.46620369, \quad -0.43236573)$
Star 3	1	$(-0.97000436, \quad 0.24308753)$	$(-0.46620369, \quad -0.43236573)$

Using these initial conditions, the motion of the three stars is periodic, as can be seen again in the corresponding animation. To illustrate this, we plot the trajectories at time $t = 40$ (we choose a longer time interval than in the previous case to better visualize the periodic behavior). The three stars move along the following paths

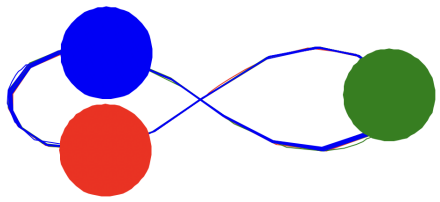

Figure 2: Plot of the final trajectories of the stars for the chosen initial conditions. The motion is now periodic as expected.

Hence, we can clearly see that the motion is now periodic, as expected.

3 Exercise 2: The Orbit of a Supermassive Black Hole Binary

We aim to integrate the orbit of a supermassive black hole (BH) binary subject to dynamical friction. The equation of motion for a black hole is

$$\frac{d^2\mathbf{r}_{\rm BH}}{dt^2} = -\frac{GM_{\rm BH}}{4r_{\rm BH}^3}\mathbf{r}_{\rm BH} + \dot{\mathbf{v}}_{\rm DF}, \tag{23}$$

where the last term on the right-hand side represents the force due to dynamical friction (DF). We approximate this force as

$$\dot{\mathbf{v}}_{\rm DF} = -\frac{A}{v_{\rm BH}^3 + B}\mathbf{v}_{\rm BH}, \tag{24}$$

where A and B are constants representing, respectively, the product of the black hole mass with the stellar density, and the cube of the velocity dispersion of the surrounding stellar field. The objective of this problem is to determine whether the BH binary can approach close enough at pericenter to lose energy through gravitational radiation. This occurs when $r_{\rm peri} \sim r_s$, the Schwarzschild radius. For the calculation, we set $M = G = 1$ and adopt a unit of distance of 100 parsecs. In these units, the Schwarzschild radius is

$$r_s = 10^{-7}. \tag{25}$$

We will use a fourth-order Runge–Kutta integrator with adaptive time steps, as employed in the previous exercise, to perform this calculation. Furthermore, since the orbit is symmetric (i.e., the black holes are identical), it is sufficient to solve for the position of only one black hole.

3.1 Solution Question a

In this part, we solve the problem without including dynamical friction and aim to determine a reasonable value for δ, which represents the error tolerance per unit time necessary for applying the adaptive step-size method. To do this, we start with a trial value, in our case $\delta = 10^{-7}$, and verify that, when solving the orbit without dynamical friction and setting the initial velocity such that $r_{\rm peri} = 10^{-7}$, there is no appreciable loss of accuracy over at least 10 orbits.

So first of all we have computed the initial velocity such that $r_{\rm peri} = 10^{-7}$, just by trial and looking if the pericenter is 10^{-7}. Doing this we found that a reasonable value of the initial velocity is

Table 3: Initial conditions for the black hole.

Mass	Initial Position (x, y)	Initial Velocity (v_x, v_y)
1	(1, 0)	(0.0, 0.00023)

In this way, by integrating Eq. (23) with $A = B = 0$ (i.e., without dynamical friction) using a Runge-Kutta method with adaptive step size, from time $t = 0$ up to $t = 50$ (sufficient to observe at least 10 orbits), we obtain the following orbit

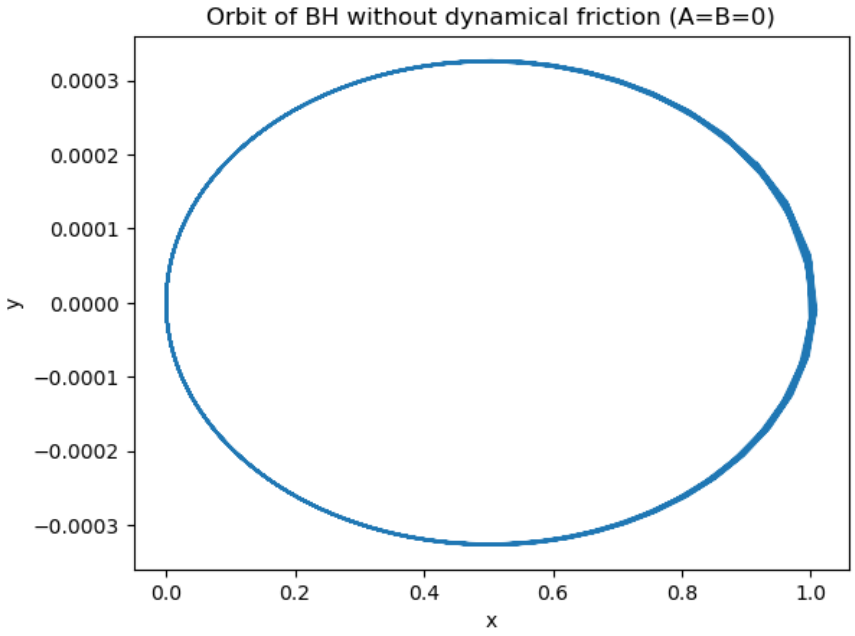

Figure 3: Plot of the orbit in the case of $A = B = 0$.

From this, we immediately see that, since the system evolves without dynamical friction, the orbit of the black hole remains stable. Therefore, we expect the energy to be conserved, varying only very slightly, and similarly the orbital radius, defined as $r = \sqrt{x^2 + y^2}$, remains almost constant over at least 10 orbits. Indeed, considering the relative energy variation, defined as

$$\delta E_r = \frac{\Delta E}{E(t=0)} = \frac{E(t) - E(t=0)}{E(t=0)}, \tag{26}$$

and plotting it as a function of time, over the interval corresponding to 10 orbits, we obtain

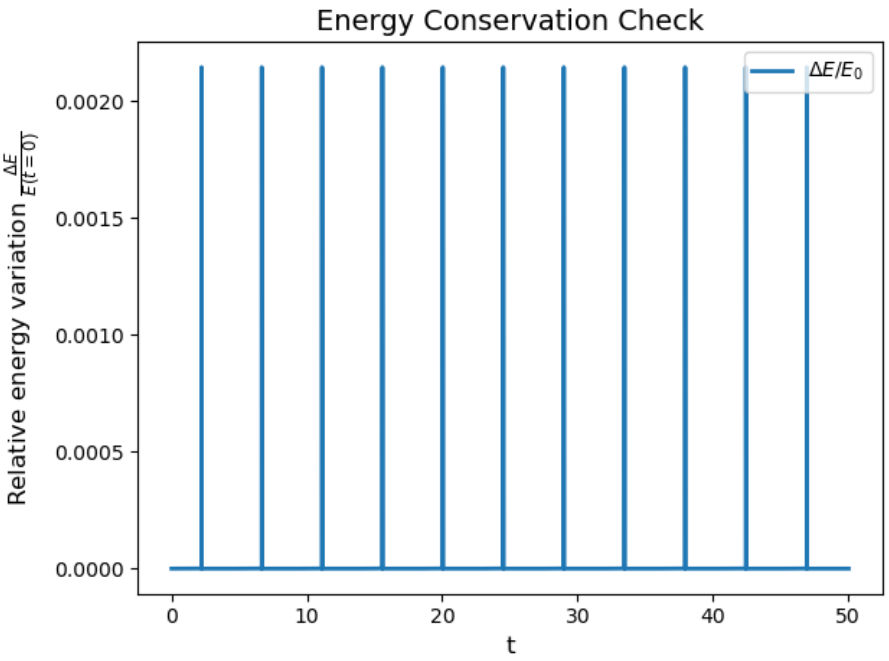

Figure 4: Relative variation of the energy as a function of time.

We observe that the maximal relative variation is at most $\delta E_r \sim 0.0021$, i.e., of the order of 10^{-3}. Therefore, we verify that the relative variation of the energy does not change significantly over 10 orbits.

Similarly, by plotting the behavior of the radius r (defined previously), we observe that

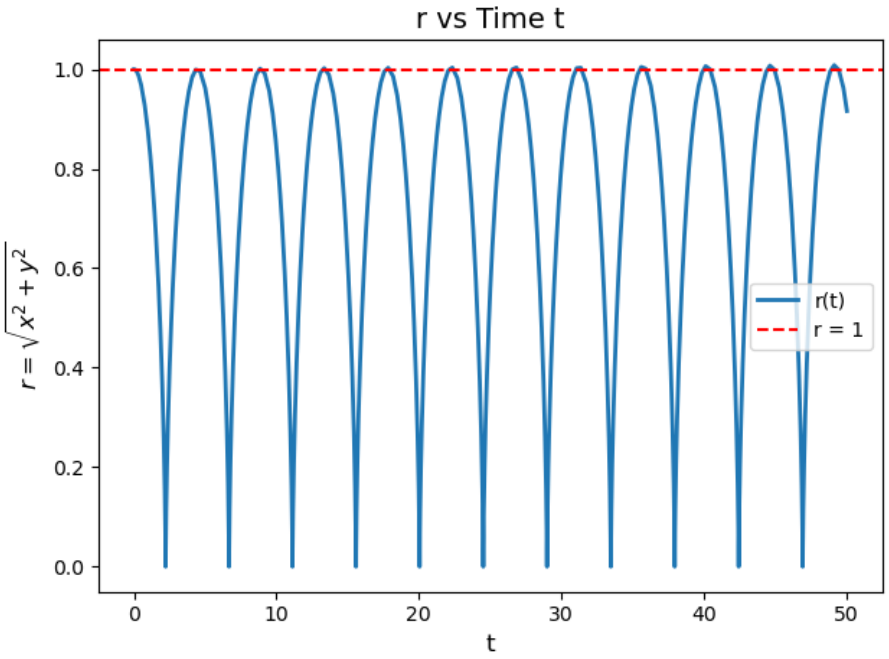

Figure 5: Radius r for $A = B = 0$ as a function of time. The dashed red line indicates the initial value of r.

From this, we see that at the end of each period the radius is exactly the same as its initial value, which in

our case is $r = 1$, confirming that the orbits are stable and that there is no appreciable loss of accuracy over at least 10 orbits. This also confirms that our initial choice of $\delta = 10^{-7}$ is reasonable, and we will use this value throughout the homework.

3.2 Solution Question b

We now consider the case with dynamical friction, taking in particular $A = B = 1$. We want to plot the orbit in this case and study the behavior of the radius $r = \sqrt{x^2 + y^2}$. The integration is stopped when r reaches the pericenter, $r_{\rm peri} = 10^{-7}$. By implementing the same algorithm as in the previous case, but now solving the full Eq. (23), and with the following initial condition

Table 4: Initial conditions for the black hole in the case $A = B = 1$.

Mass	Initial Position (x, y)	Initial Velocity (v_x, v_y)
1	(1, 0)	(0.0, 0.00023)

where the initial velocity is obtained by the question to be

$$v_0 = 0.8 \cdot v_{circ} = 0.8 \cdot \sqrt{\frac{1}{4r}}, \tag{27}$$

But since $v_{\rm circ}$ is the velocity of circular orbits, we can choose any value of r; therefore, we simply take $r = 1$, and we obtain the results shown in Tab. 4. So, in the end, we obtain the following black hole orbit

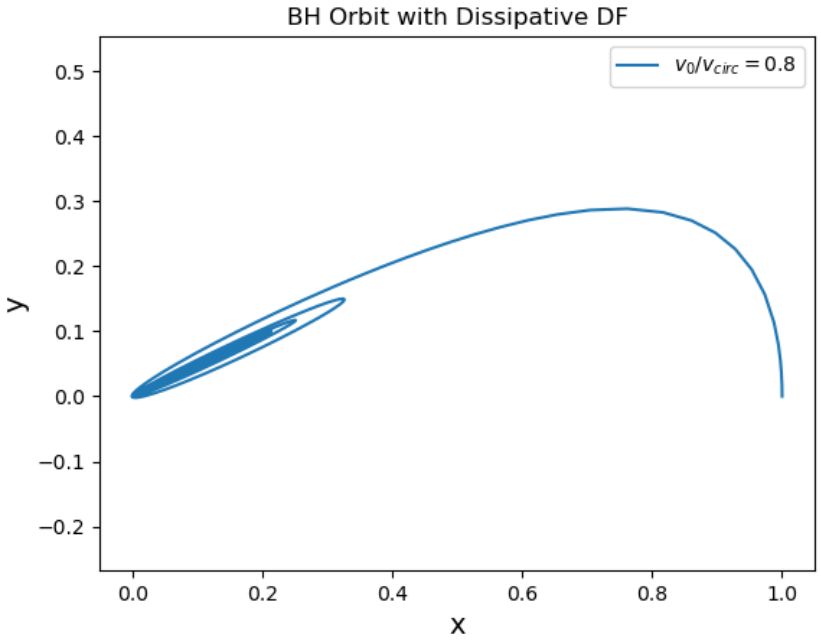

Figure 6: Plot of the orbit in the case of $A = B = 1$.

We can clearly see that the orbit is no longer elliptical; instead, the black hole begins to spiral inward. To further confirm the behavior observed from the orbit, we plot the logarithm of the radius r as a function of time; we then obtain

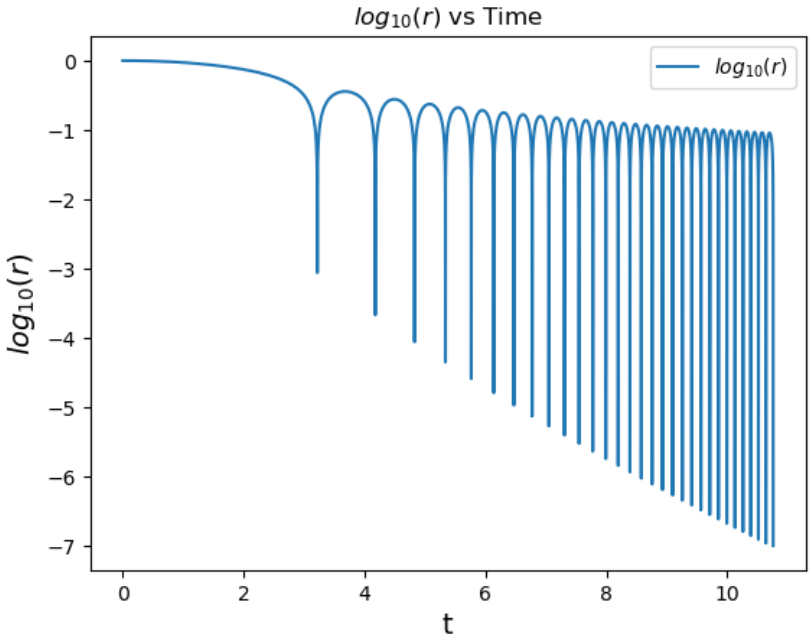

Figure 7: Plot of the logarithm of the radius r as a function of time.

We also computed the total time that the black hole need to achieve the value of $r = 10^{-7}$, and we found that it is

$$t = 10.76. \tag{28}$$

3.3 Solution Question c

We are now interested in understanding how the time required for the black hole to reach the Schwarzschild radius depends on the parameters that enter the dynamical friction term. In particular, we focus on the dependence on the ratio B/A. To investigate this, we perform simulations varying A and B while keeping the initial velocity fixed, and we record the time at which the black hole reaches $r = r_{\rm s}$, which, as a reminder, corresponds to the pericenter radius. First of all, we need to understand how to express the time in units of Myr. In units where $G = M = 1$, since

$$G \sim \frac{(\text{length})^3}{(\text{mass}) \cdot (\text{time})^2}, \tag{29}$$

and considering that distances are measured in units of 100 pc, it follows that in these units, time is dimensionless. Indeed, so far we have not used any physical units for time.

Now, if we denote by $r_{\rm sim} = 10^{-7}$ the radius used in the simulation (in units with $G = M = 1$), and by $r_{\rm phys}$ the corresponding physical radius in distance units, we have

$$r_{\rm phys} = L_0\, r_{\rm sim}, \tag{30}$$

where $L_0 = 100\,\text{pc}$ is the conversion factor for distance. Similarly, we can define a conversion factor for mass, which we call M_0, so that

$$M_{\rm phys} = M_0\, M_{\rm sim}. \tag{31}$$

Since in the simulation units $M_{\rm sim} = 1$, we have $M_{\rm phys} = M_0$. On the other hand, the physical mass can be obtained from

$$M_0 = M_{\rm phys} = \frac{c^2\, r_{\rm phys}}{2G} = \frac{c^2\, r_{\rm sim} L_0}{2G}, \tag{32}$$

and since the conversion factor for time is

$$t_0 = \sqrt{\frac{L_0^3}{GM_0}}. \tag{33}$$

substituting the previous expressions, we obtain

$$t_0 = \frac{L_0}{c}\sqrt{\frac{2}{r_{\rm sim}}} \simeq 1.458\,{\rm Myr}. \tag{34}$$

Thus, to convert time into Myr, we must multiply by t_0.

Now, using the same initial conditions as before, by plotting the time required for the black hole to reach the Schwarzschild radius (converted to Myr) as a function of the ratio B/A, with $A, B \in [0.5, 10]$, we obtain

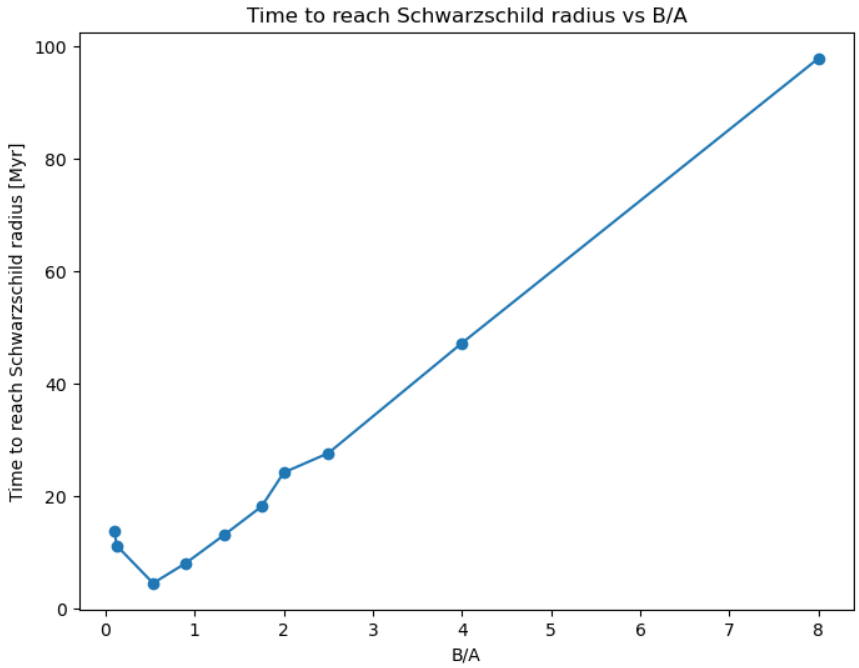

Figure 8: Time to reach the Schwarzschild radius as a function of the ratio B/A.

We see that for $B/A \gg 1$, the time also increases. This makes sense, since, by looking at Eq. (23), in this regime the friction effectively become negligible: for larger ratios, the friction is smaller, and the time required to reach the Schwarzschild radius becomes longer.

3.4 Solution Question d

So far, we have not yet understood whether the time to reach the Schwarzschild radius depends on the individual values of A and/or B. To investigate this, starting from the initial conditions in Tab. 4, we plot the desired quantity for a fixed value of A while varying B. The resulting plot is shown below

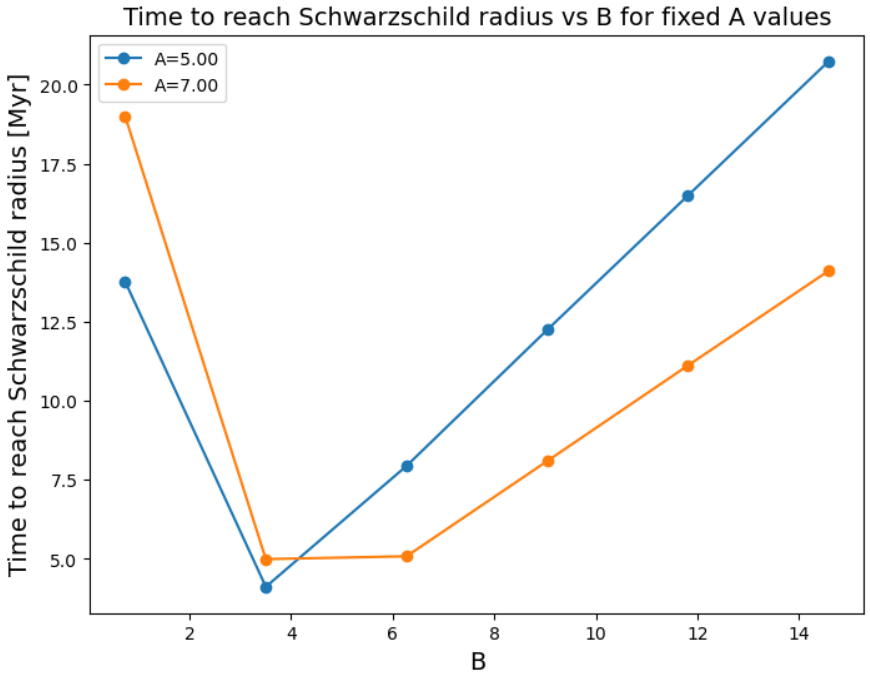

Figure 9: Time to reach the Schwarzschild radius as a function of the ratio B and A individually.

We see that the time depends on both A and B: for a fixed B, the time needed to reach the Schwarzschild radius changes varying A, and for a fixed A with changing B, the behavior is also different. This behavior makes sense since, for small B, from Eq. (23) we have

$$\dot{\mathbf{v}}_{\rm DF} = -\frac{A}{v_{\rm BH}^3 + B}\mathbf{v}_{\rm BH} \simeq -\frac{A}{v_{\rm BH}^3}\mathbf{v}_{\rm BH}, \tag{35}$$

so the dynamical friction is small and the time increases. When B is large, the same should happen: the dynamical friction becomes negligible and the time grows. This is what is observed in the graph reported.

In the end, we can also see the dependence of our results on the initial velocity. Therefore, we first plot the time required to reach the Schwarzschild radius as a function of different initial velocities, and we obtain

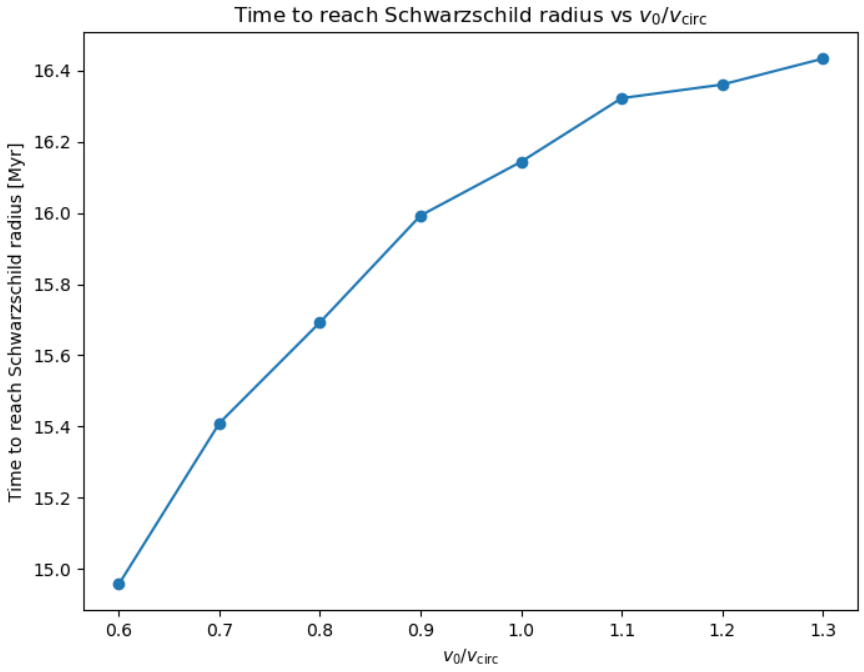

Figure 10: Time to reach the Schwarzschild radius as a function of the ratio v_0/v_{circ}.

We see that, as the ratio increases, the time required to reach the Schwarzschild radius also increases, since the drift becomes smaller. Another plot we made shows the different orbits as a function of the initial velocity, and we obtain

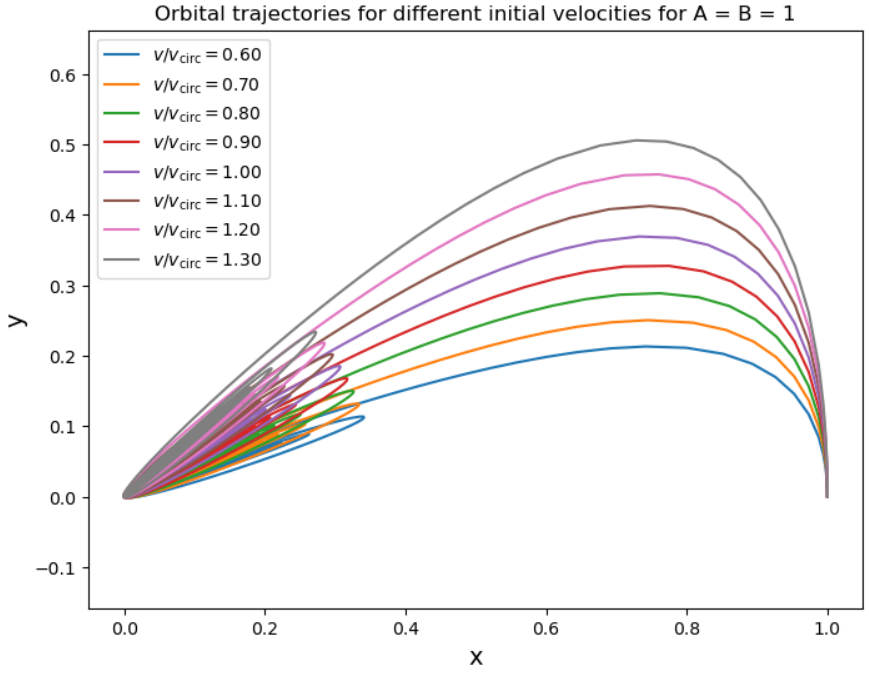

Figure 11: Different orbits as a function of the ratio v_0/v_{circ}.

We can clearly see the dependence on the initial velocity: a larger initial radius corresponds to a longer time,

also since the trajectory is larger. In the end, we find that our results depend individually on the initial velocity v_0, on the individual values of A and B, and of course on the ratio B/A. This answers our question.

4 Conclusion

Finally, in this homework we understood how the Runge–Kutta method works at fourth order by examining two applications: the simulation of the three-body decay and the computation of the orbits of a supermassive black hole binary in the presence of dynamical friction. We observed how the initial conditions play an important role in both problems, and how to implement adaptive step size, which is also crucial for many physical problems.

5 Code

The code containing all the results can be found at the following Repository GitHub.